

# Advances in Biological Structure, Function, and Physiology Using Synchrotron X-Ray Imaging\*

Mark W. Westneat,<sup>1,†</sup> John J. Socha,<sup>2</sup>  
and Wah-Keat Lee<sup>2</sup>

<sup>1</sup>Department of Zoology, Field Museum of Natural History, Chicago, Illinois 60605; email: mwestneat@fieldmuseum.org

<sup>2</sup>Advanced Photon Source, Argonne National Laboratory, Argonne, Illinois 60439; email: jjsocha@aps.anl.gov, wklee@aps.anl.gov

Annu. Rev. Physiol. 2008. 70:119–42

The *Annual Review of Physiology* is online at <http://physiol.annualreviews.org>

This article's doi:  
10.1146/annurev.physiol.70.113006.100434

Copyright © 2008 by Annual Reviews.  
All rights reserved

0066-4278/08/0315-0119\$20.00

\*The U.S. Government has the right to retain a nonexclusive, royalty-free license in and to any copyright covering this paper.

†To whom correspondence should be addressed.

## Key Words

imaging, CT, biomechanics, morphology, respiration, feeding, insects

## Abstract

Studies of the physiology and biomechanics of small (~1 cm) organisms are often limited by the inability to see inside the animal during a behavior or process of interest and by a lack of three-dimensional morphology at the submillimeter scale. These constraints can be overcome by an imaging probe that has sensitivity to soft tissue, the ability to penetrate opaque surfaces, and high spatial and temporal resolution. Synchrotron X-ray imaging has been successfully used to visualize millimeter-centimeter-sized organisms with micrometer-range spatial resolutions in fixed and living specimens. Synchrotron imaging of small organisms has been the key to recent novel insights into structure and function, particularly in the area of respiratory physiology and function of insects. X-ray imaging has been effectively used to examine the morphology of tracheal systems, the mechanisms of tracheal and air sac compression in insects, and the function of both chewing and sucking mouthparts in insects. Synchrotron X-ray imaging provides an exciting new window into the internal workings of small animals, with future promise to contribute to a range of physiological and biomechanical questions in comparative biology.

**Biomechanics:** the study of organisms from the perspectives of physics and engineering

**Computed tomography (CT):** an imaging method that uses multiple two-dimensional images to create a three-dimensional visualization of an object or organism

**Synchrotron:** an accelerator in which charged particles move in a circular path, using electromagnetic fields

**X-ray:** a relatively high-energy photon or stream of such photons having a wavelength in the approximate range from 0.01 to 10 nanometers; used for its penetrating power in radiography and scientific imaging

**Phase-contrast imaging:** a process that uses the differences in the phase of light transmitted or reflected by a specimen to form distinct, contrasting images of different parts of the specimen

**Resolution:** the fineness of detail that can be distinguished in an image

**Density:** a measure of how much mass is contained in a given unit volume, related to image intensity in X-ray imaging

## INTRODUCTION: SYNCHROTRON X-RAY IMAGING FOR BIOLOGY

Throughout the history of biology, advances in the visualization of biological structures and organic processes have transformed our understanding of anatomy, physiology, and evolution. The ability to view and record the structure and motion of internal anatomical systems as well as whole-animal behavior in living organisms is essential to comparative physiology, biomechanics, and medicine. For morphologists, new techniques in microscopy such as scanning and transmission electron microscopy (1), confocal fluorescence microscopy (2), and computed tomography (CT) (3) have yielded many discoveries in anatomical disciplines. Similarly, new ways of imaging the real-time motion of living organisms, such as high-speed video (4), have greatly accelerated our understanding of the fundamental principles of animal function. The development of synchrotron X-ray sources and phase-contrast imaging techniques (5, 6) has resulted in major advances in both the microscopic imaging of preserved specimens and the real-time X-ray video of the internal processes of living organisms. The goal of this review is to present the utility of synchrotron X-ray imaging for anatomical and physiological investigations and emphasize how the improved ability to see inside small organisms enables biologists to answer important questions in functional and comparative biology.

Such techniques for viewing internal anatomical structures and physiological processes in living organisms have led to important discoveries in animal locomotion (7), feeding (8), and respiration (9). However, real-time visualization of the internal processes of small animals has been limited by scaling factors and imaging technology. To visualize internal physiological mechanisms in real time, an imaging tool must have the ability to penetrate the opaque exterior of an organism, spatial resolution in the 1–10- $\mu$ m range, temporal resolution of less than 100 ms,

and the appropriate sensitivity of image range to distinguish among soft tissues. For small moving animals, various limitations of resolution, surface penetration, and imaging duration often combine to make visible light microscopy (conventional or confocal), near-infrared (NIR) microscopy (10), magnetic resonance (11), and ultrasound (12) insufficient for real-time functional imaging.

Recently, synchrotron X-ray phase-contrast imaging (13–15) has been shown to be ideal for visualizing well-defined internal structures that have different mass densities, including a wide range of biological tissue types and organ systems in both plants and animals. This review presents the basic principles and technical approaches to synchrotron X-ray imaging and outlines the many uses for anatomical imaging, applications in micro-CT imaging, and the analysis of physiological and biomechanical processes in living organisms.

### Synchrotron X-Ray Imaging: Techniques, Sources, and Analysis

Imaging is the oldest application of X-rays: The original discovery of X-rays came about from images formed on a photographic plate. When an electromagnetic wave such as an X-ray passes through a noncrystalline sample, two things happen: The amplitude of the wave is attenuated as a result of absorption by the sample, and the wave front becomes distorted because the wave travels at different speeds through different materials. In conventional X-ray imaging, contrast is due solely to the differences in absorption within the sample (e.g., bone and tissue). However, most biological samples are composed largely of water and therefore do not produce usable imagery because of insufficient contrast. The advent of X-ray phase-contrast techniques (16) in the mid-1990s greatly changed this because phase-contrast techniques are sensitive to the distortions in the transmitted X-ray wave front. As a result, even samples with

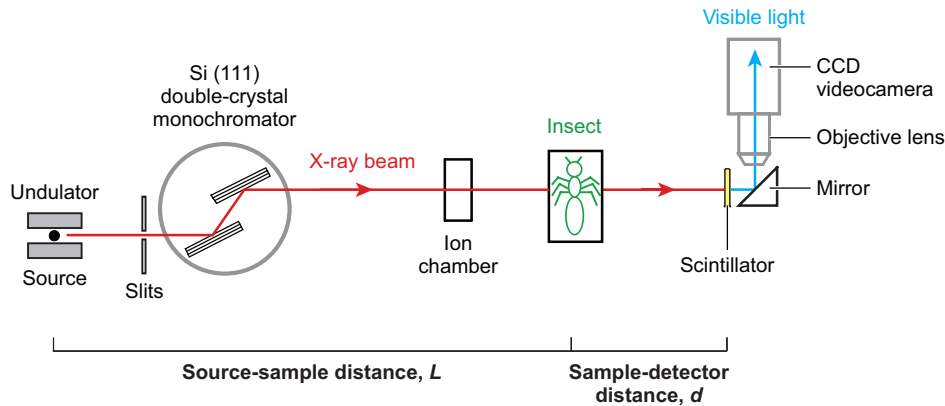


**Figure 1**

X-ray phase-contrast imaging diagram (14). X-rays are produced by an undulator and are monochromatized by a double-crystal monochromator. The X-rays pass through an ion chamber and then the sample and are converted to visible light by a scintillator screen. A digital imaging sensor records the resulting image. For anatomical and computer tomographic (CT) imaging, high-resolution cameras are used. In contrast, living, behaving organisms are recorded through the use of standard digital video (30 Hz) or light-sensitive high-speed video imaging systems. The source-sample distance ( $L$ ) is a characteristic of the beamline, and the sample-detector distance ( $d$ ) is set by the experimenter to optimize phase enhancement. CCD denotes charge-coupled device.

minute absorption differences can be clearly visualized, allowing for the recent advances in X-ray imaging for small biological samples. The term phase contrast has been used to include dramatically different techniques with different sensitivities to wave-front distortions. In this review, we focus on the simplest (and, as a result, the most frequently applied) of these techniques, which is sometimes called propagation-based phase contrast.

At a synchrotron facility, electrons traveling near the speed of light are maintained in a storage ring by electromagnetic fields. When the electrons are accelerated by changing the direction of travel, X-rays are emitted. This acceleration is produced by bending magnets that are used to maintain the electrons in a circular orbit or by special magnetic insertion devices that are designed to increase the X-ray beam intensity dramatically. The basis of X-ray phase-contrast imaging is Fresnel diffraction (**Figure 1**). After passing through a specimen of interest, the X-ray image is created, at the focal plane of the scintillator, by the interference of the diffracted components of the beam with itself and the nondiffracted part of

the beam. Interfaces between materials with different densities correspond to discontinuities in the refractive index, causing Fresnel diffraction to occur and rendering the tissue interfaces as high-low intensity fringes in the images (17). This edge-enhancement effect is one of the key features of synchrotron imaging because it improves the sensitivity of imaging structures with only small density differences and absorption contrast (15).

Compared with conventional laboratory-based X-ray sources, synchrotrons have the advantages of a wide energy range, a high photon flux, and good beam coherence. The wide energy range enables a wide range of samples to be studied. The high photon flux, typically  $10^6$ – $10^9$  times higher than laboratory-based sources, enables fast acquisition times and high-speed imaging. The beam coherence permits phase techniques to be implemented. The field of view in synchrotron imaging is a function of the beamline and detector. In practice, the ratio of the field of view to achievable or maximum resolution is limited by the detector pixel number. Nanometer-scale resolutions are possible with micron-scale

**Absorption contrast:** the visible difference between materials in an X-ray image due to differences in the electron density of the materials (e.g., bone and soft tissue)

**Fresnel diffraction:** near-field diffraction, a process of diffraction that occurs when a wave passes through an aperture and diffracts in the near field, causing any diffraction pattern observed to differ in size and shape, relative to the distance

---

**Edge enhancement:** an effect in phase-contrast imaging whereby the edges of objects become highlighted relative to one another

**SR- $\mu$ CT:** synchrotron radiation microscopic computed tomography

---

images. For example, 3-D renditions of a single yeast cell have been achieved at 60 nm with synchrotron radiation microscopic computed tomography (SR- $\mu$ CT) (18) and at 30 nm with diffraction microscopy (19). Spatial distributions of trace metals within a cell can be imaged with <200-nm spatial resolution (20). These advantages permit unprecedented X-ray imaging of millimeter-sized biological specimens with micrometer to submicrometer spatial resolution and submillisecond temporal resolution.

Although raw X-ray images are 2-D projections of a 3-D sample along the beam direction, CT can yield 3-D renditions of the sample. This nondestructive technique has revolutionized biomedical imaging and has provided scientists with clear 3-D views of the internal structure of many organisms without resort to histology or dissection. CT analysis is applicable to both absorption-contrast or phase-contrast X-ray data, and in many cases, phase-contrast data are used with absorption-only CT algorithms to produce 3-D renditions (15). Because the phase information is not included in the algorithm, the image intensity values do not map one to one with density. However, the resulting images contain rich data on morphology, tissue composition, and quantitative information on length, area, and volume.

This review focuses on imaging millimeter-sized anatomy and physiology with micrometer-scale resolution, with an emphasis on real-time measurements in living specimens. For imaging of preserved or nonliving specimens, image quality may be optimized for the particular contrast level desired. However, for *in vivo* applications, the use of longer X-ray wavelengths results in higher absorption, which is detrimental to living organisms. Similarly, higher beam intensities yield brighter and less noisy images but will cause more harm to a living organism, requiring effort to optimize synchrotron phase-contrast imaging for organismal studies (14). Below, we first show the insights that may be gained into

structure and function through the use of imaging of preserved or nonliving tissues. We then discuss physiological results from experiments with living animals and finally highlight recommendations for optimizing imaging and survivorship.

## ANATOMICAL IMAGING USING COMPUTED TOMOGRAPHY

Major advances in resolution and ease of use of SR- $\mu$ CT for the imaging of biological materials (5, 6) enable biologists to section samples virtually in any direction, in their natural state, and without dissection or histology (15). Other benefits are that a wide range of density differences are detected so that soft tissue such as muscles (15), nerves (21), plant tissues (22), and the digestive tract (23) can be displayed. Several reviews of X-ray CT using synchrotron radiation have highlighted the use and the physical principles of SR- $\mu$ CT and its benefits as a noninvasive imaging technique (15, 22–32). Here we highlight the wide range of anatomical insights for function and development that have been gained through the use of this technique.

At the whole-organism level, the recent application of SR- $\mu$ CT to insect anatomy (15) demonstrated the ability to visualize fine details of the complex musculature in insect heads with diameters of approximately 0.5 mm, illustrated in various planes of section (**Figure 2a,b**) as well as 3-D reconstructions of the entire head (**Figure 2c**). The contrast between the different tissues in the CT images was also sufficient to distinguish between cuticular structures and soft tissues such as muscle and nerve tissue (**Figure 2c**). CT sections were well suited for anatomical analysis of complex body structures, such as the origin and insertion of the many cephalic muscles, visualized by moving back and forth within the 2-D image stacks or by cutting into the reconstructed 3-D volume models. These fine details of insect cephalic morphology represent important data for comparative and evolutionary analyses of insect

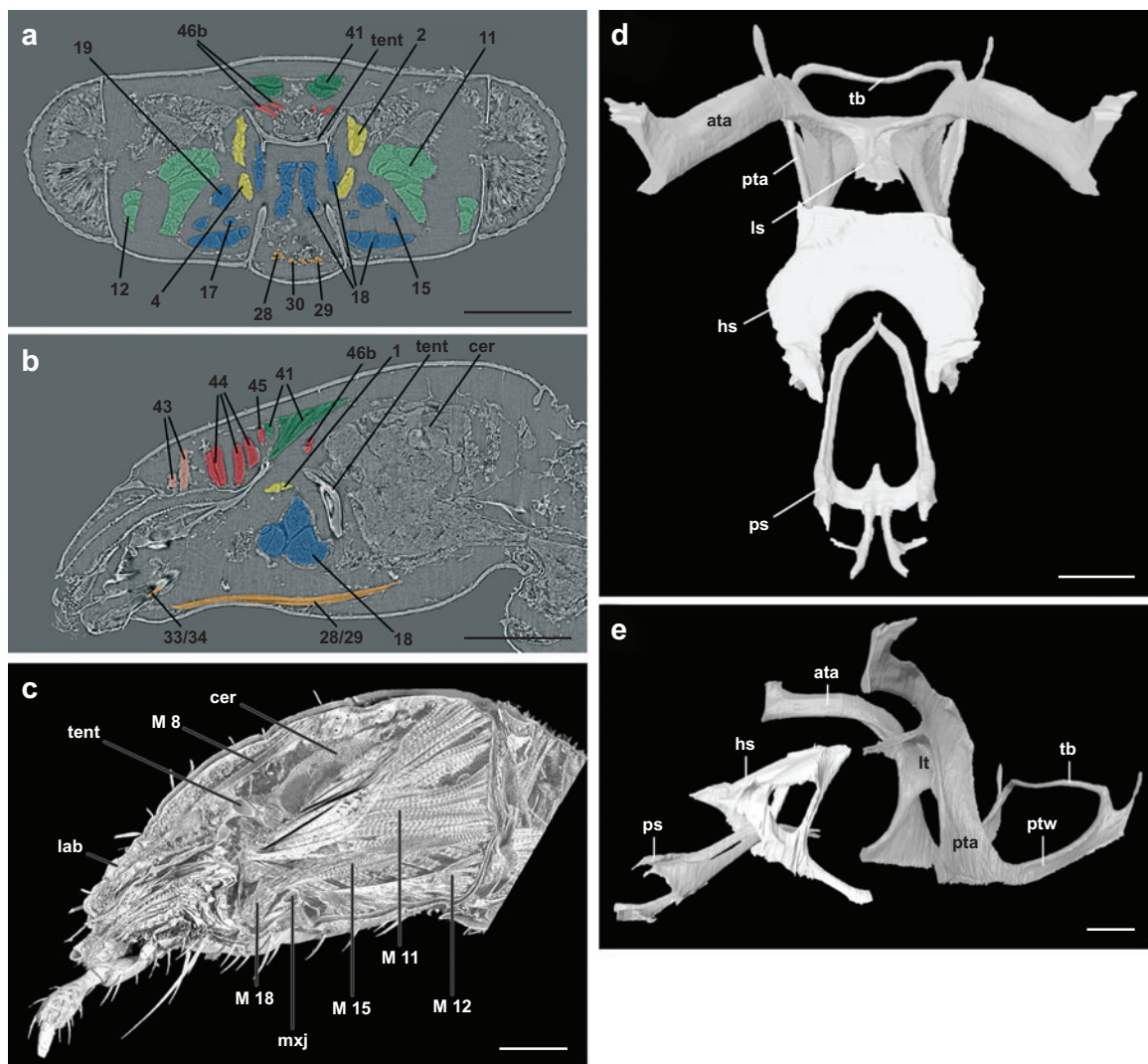


**Figure 2**

SR- $\mu$ CT images of rove beetles (family Staphylinidae) (15). Virtual sections in the (a) transverse plane and (b) sagittal plane through the head of *Gyrophaena fasciata*. Colors identify functional groups of muscles: yellow, antennal; red and pink, pharyngeal; orange, labial; light green, mandibular; dark green, hypopharyngeal; and blue, maxillary. (c) 3-D model of the head of *Gyrophaena gentilis* with the left part of the head cut off to view inside the head capsule. Note the striation of the muscles, which indicates that the effective pixel size is less than 3  $\mu$ m. (d) Frontodorsal and (e) lateral 3-D rendering of *G. fasciata*, in which the sclerites of the hypopharynx (white) and prementum (bright gray) complex are shown in relation to the tentorium (dark gray). Abbreviations used: ata, anterior tentorial arm; cer, cerebrum; hs, hypopharyngeal sclerite; lab, labrum; ls, lamellose structure; lt, laminatentorium; mxj, maxillary joint; ph, pharynx; ps, praementum sclerite; pta, posterior tentorial arm; ptw, posterior tentorial wall; tb, tentorial bridge; tent, tentorium. Muscles denoted by numbers (see Reference 15 for details). Scale bars = 100  $\mu$ m.

structure and for biomechanical analyses of feeding mechanisms.

Anatomical and functional analysis using SR- $\mu$ CT also revealed the 3-D morphology of the sponge *Tethya wilhelma* (33). The organization of the sponge's living tissue, mineralized skeleton, and water transport system was analyzed to generate a complete view of the canal network and water-flow systems (Figure 3*a,b*). This investigation revealed that bypass canals may function to

lower pressure pulses during contraction and that recirculation channels may make nutrient uptake more efficient. X-ray tomography has also advanced embryological research on both plants and animals. Application of SR- $\mu$ CT to the seeds of the important genetic model plant species *Arabidopsis thaliana* (22) recently revealed a complex network of air spaces between the cell walls within the seed (Figure 3*c,d*). This work produced high-resolution images of the embryonic plant in a

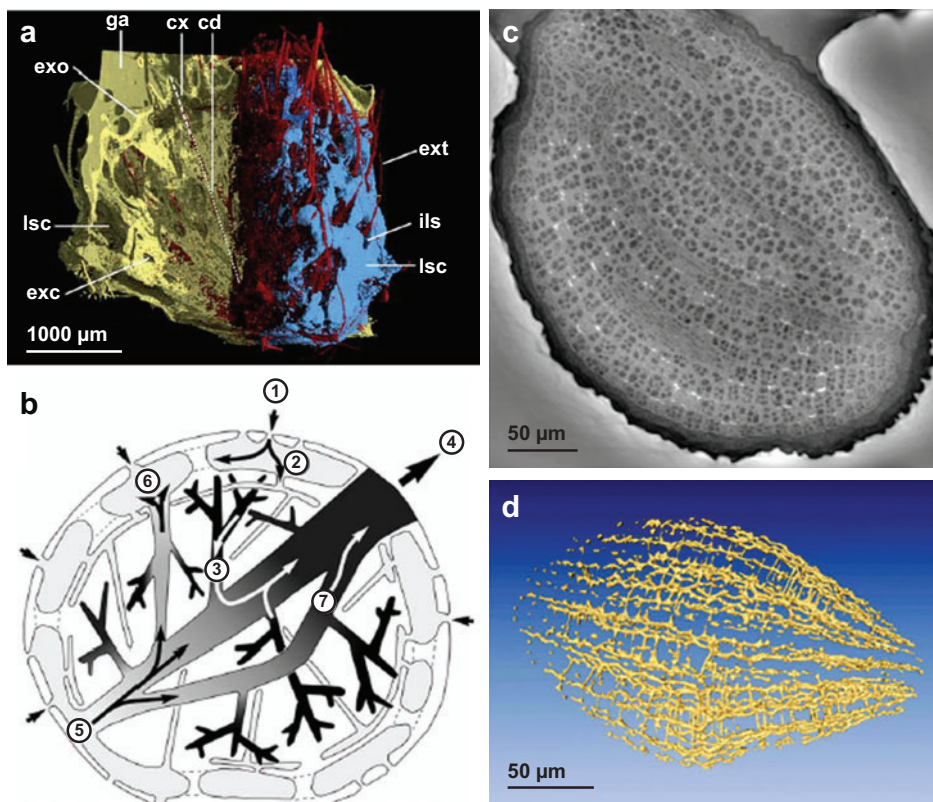


**Figure 3**

SR $\mu$ CT of sponge and seed tissues. (a) Stereo pair rendering of the sponge *Tethya wilhelma* (33): sponge tissue (yellow), skeleton (red) and aquiferous system (blue), choanoderm (cd), ortex (cx), glue artifact (ga), excurrent canal (exc), exopinacoderm (exo), body extension (ext), interlacunar space (ils), lacunar system cavity (lsc). (b) Schematic representation of the aquiferous system of *T. wilhelma* (33). A proposed hypothetical flow regime, indicated by arrows and numbers, includes incurrent water through ostia (1) into the sublacunar system (2), passage through the choanocyte chambers into the excurrent canals (3), expulsion through the oscule (4), alternative flow directly from the lacunae into the main excurrent canal (5), reflux into the lacunae through bypass canals (6), and recirculation or alternative routes through the anastomosing main excurrent canal (7). (c) Architecture of an *Arabidopsis thaliana* seed reconstructed by quantitative phase tomography, with virtual slice through the seed, 0.3  $\mu$ m thick (22). (d) A 3-D rendering of the intercellular air space network in the hypocotyl of the *Arabidopsis* seed (22).

mature seed, providing new structural details of the cotyledons, hypocotyl, and radicle components of the *Arabidopsis* embryo. A previously unidentified void network of air spaces, which formed an interconnected network of air channels throughout the hypocotyl cortex, was discovered throughout the seed tissues (Figure 3*d*). This network may be involved in oxygen supply during the early stages of seed germination and in rapid water transport. X-ray imaging of plant tissues has also been performed as a way to identify the location and genetic control of iron deposition in seeds (34) and the distribution of various metals in plants (35, 36).

The X-ray microscopy of fossils using synchrotron radiation has been an area of active research, with investigation of organisms ranging from fossil plants (37) to fossil arthropods (38), primate teeth (39), fossilized bone (40), and ancient metazoan embryos (41, 42). Perhaps most strikingly, synchrotron X-ray imaging has revealed the microstructure of embryos from deep evolutionary time (41). Fossilized embryos of early metazoan forms from the Proterozoic, more than 500 mya, hold many clues to early developmental features. The details of the internal morphology of embryos from several lineages, reconstructed in 3D, helped to clarify their phylogenetic affinities and shed new light on germ layer formation in early metazoans. A large number of other investigations have used SR- $\mu$ CT to explore anatomical, functional, or developmental features of organic tissues, including the ultrastructure of sea urchins (43, 44), the circulatory system of the woodlouse (45), the morphology of snails (46, 47), the inner ear and cochlea of mammals (48), the pathways of nerves (49), and the vascular networks of the brain (50).

## REAL-TIME X-RAY VIDEO OF INTERNAL FUNCTION

Analysis of the physiology and function of living organisms using synchrotron X-ray imaging began within the past decade and is quickly

developing into a powerful tool for examining the many interior mechanisms of small animals that have previously been difficult to visualize. The recent observation and quantification of rapid tracheal volume changes during respiratory ventilation in insects (13) were the first experiments in which synchrotron X-ray imaging was applied to small living animal function. These experiments demonstrated the extent to which physiology and biomechanics may benefit from this method. This section highlights the major findings of physiological and functional applications of X-ray imaging in the areas of insect respiration, feeding mechanisms of insects, functional imaging in vertebrate systems, and the trade-offs in image quality and impact of the X-rays on animals that are inherent when an imaging regime is used in a living animal preparation.

## Respiratory Mechanisms in Insects

Insects exchange carbon dioxide from the body with oxygen from the environment through a system of tracheal tubes that connects to the air via spiracles that can be actively opened or closed (51–55). Diffusion is the basis of all organismal gas exchange systems, and some insects suffice solely with this mechanism (56, 57). However, multiple additional mechanisms drive air convectively through the system (58–61), including those in which the tracheal system is actively deformed by hemolymph pressure changes, abdominal pumping, and autoventilation, during which movements of the wings or legs change the volume of tracheal air sacs (54, 62, 63). Recent research has focused on these active mechanisms for changing the volume of the tracheal system and driving gas exchange in a wide diversity of insect species. A range of recent studies (13, 14, 64–66) have used synchrotron X-ray imaging to visualize active compression and reflation cycles in the tracheal tubes and air sacs of insects and show that tracheal compressions are an important mechanism of gas exchange in some insects.

---

**Tracheae:** the internal respiratory tubes of insects and some other terrestrial arthropods

**Diffusion:** the movement of molecules in a fluid as a result of concentration differences and random thermal motion

**Convection:** the bulk flow of fluid (liquid or gas) from one area to another

**Autoventilation:** the convective movement of gas into and out of tracheal structures due to body motions such as running or flight

---



**Figure 4**

Synchrotron phase-contrast X-ray image of the tracheal system of the carabid beetle *Pterostichus stygicus* (66). (a) Head and prothorax view. (b) Zoom-in view of prothoracic tracheae (from the red box in panel a), illustrating the complex branching patterns of tracheae.

**Reynolds number:**

the dimensionless ratio of inertial to viscous forces used to characterize a flow regime

**Womersley number:**

a dimensionless number used to characterize the unsteady nature of an oscillatory or pulsatile flow

**Péclet number:** the dimensionless ratio of convective to diffusive mass transfer, relating velocity, length, and diffusion constant

The structure and respiratory function of the tracheal system of the head and thorax of several carabid beetles (ground beetles) have received intensive study recently (13, 14, 65, 66). The anterior tracheal system in these animals is complex and highly branched (**Figure 4**): Four primary tracheal trunks connect to the anterior-most pair of spiracles (**Figure 4a**) and extend anteriorly into the head after dividing into secondary, tertiary, and higher-order tracheal subdivisions (**Figure 4b**). Research on the compression patterns of tracheae in ground beetles, crickets, and carpenter ants (13) showed that rapid cycles of tracheal compression occur in these anterior sections of the tracheal system (**Figure 5**), a phenomenon not previously visible to respiratory physiologists because of the opacity of insect cuticle and the deep internal position of these tracheal systems.

More recent kinematic measurements and detailed computations of tracheal compres-

sion in both primary and secondary tracheae of the ground beetle *Platynus decentis* (65) have clarified the potential volume exchange and fluid flow properties of this behavior. During steady compression sequences, the frequency of tracheal compression was approximately 0.50 Hz, or a compression every two seconds. Kinematic analysis of the primary and secondary tracheal walls showed that the volume changes of primary and secondary tracheal tubes were 51% and 34%, respectively, meaning that a third to a half of the air in a tracheal segment flows in and out during a compression cycle (**Figure 6**). Flow velocities ranged from 0.8 to 3.3 mm s<sup>-1</sup>, implying an airflow regime with a Reynolds number of 0.01, a Womersley number of 0.03, and a Péclet number ranging from 0.005 to 0.4. These metrics of the flow regime inside a tracheal segment suggest that viscous forces dominate, turbulence is nonexistent, and diffusion is a more important process than

convection for the transport of oxygen and carbon dioxide to the tracheal wall. However, in the longer tubes that connect the head to the spiracles at the first legs, this study (65) suggested that convection plays an important role in lengthwise gas transport. The central conclusion of these studies, on the basis of visualization and measurement of respiratory mechanics, is that tracheal compression in the head and thorax may be a primary means of generating respiratory airflow in ground beetles for key tissues such as the brain, eyes, and muscles of the head.

In an additional set of respiratory experiments on the carabid beetle *Pterostichus stygicus*, X-ray videos and CO<sub>2</sub> output were recorded simultaneously for a beetle in a small respiratory chamber (66) to determine the relationship between tracheal collapse and CO<sub>2</sub> output. For comparison, CO<sub>2</sub> emission was recorded both before and after X-ray visualization took place (Figure 7). Results showed conclusively that for each tracheal compression, a corresponding pulse of CO<sub>2</sub> occurred. Such pulses can also be seen in the traces from both prior to X-ray exposure and after X-ray imaging, indicating that tracheal compressions also occurred in the absence of X-rays. The central conclusion of this work is that tracheal compressions are associated with CO<sub>2</sub> expulsion on a one-to-one basis, providing strong support for the idea that compressions are a mechanism of convective gas exchange in some carabid beetle species.

The convective respiratory behavior of insects with air sacs has also been studied in several taxa, including flies, bees, and grasshoppers. Gas exchange using air sacs in the head, thorax, or abdomen is usually driven by active mechanisms such as abdominal pumping and autoventilation. Abdominal pumping is widespread in insects (61, 62), and recent experiments on the respiratory function of this behavior have been performed on grasshoppers (67, 68), lepidopterans (62, 69), ants (70), and other insects. Autoventilation is often associated with running or flying, during which movements of the abdomen, thoracic walls,

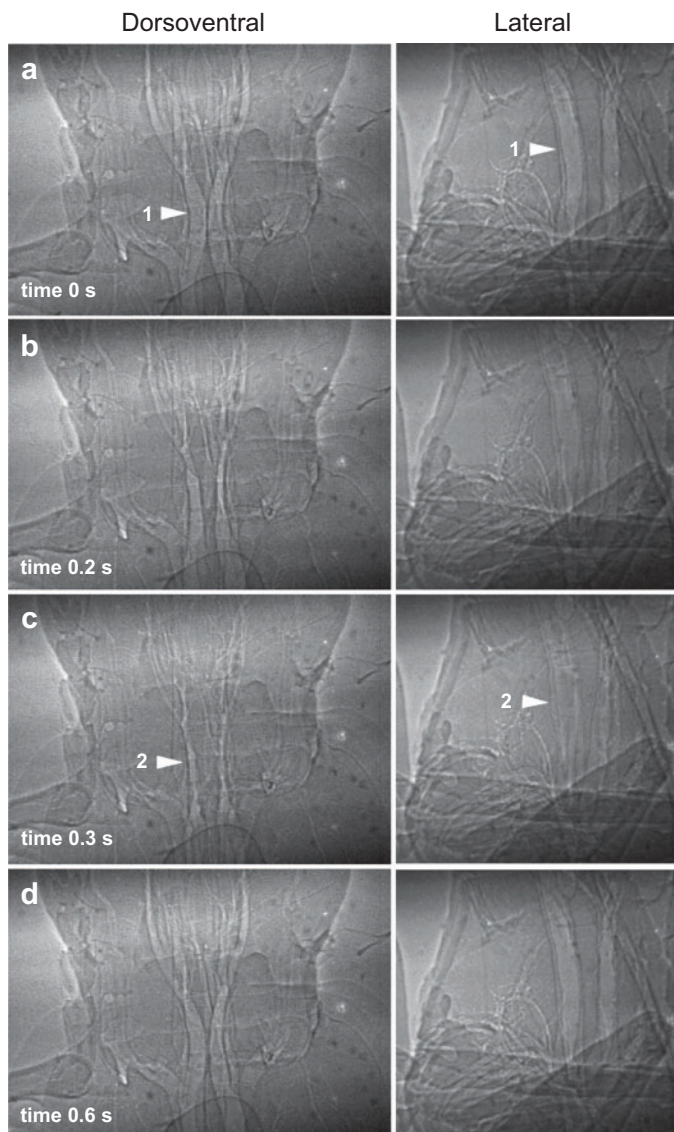


**Figure 5**

Respiration by tracheal compression in the head and thorax of the beetle *Platynus decentis* (13). The left panels (3 mm wide) show a dorsoventral view (head, up; sides, left and right), and the right panels show a lateral view (head, up; ventral, left) of a different beetle. Tracheal tubes are expanded at rest (a, arrow 1), and compression (b) occurs throughout the anterior region of the insect. Lateral compression results in narrower tracheae in the dorsal view and wider tracheae in the lateral view. Maximal compression (c, arrow 2) is followed quickly by expansion of tracheae (d), with the entire compression-and-expansion cycle completed in less than 1 s.

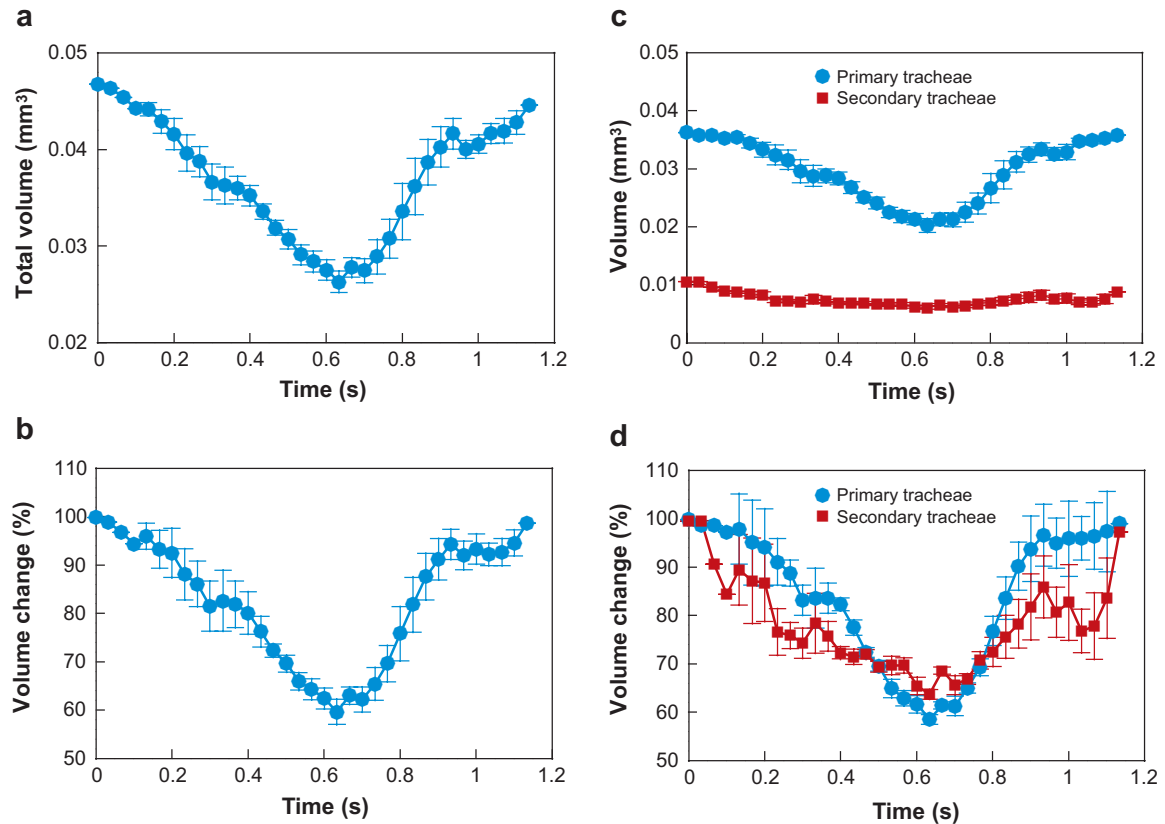


**Figure 6**

Representative profiles of volume change in the primary and secondary tracheae of a single individual ground beetle (*Platynus decentis*) (65). All plots are the mean of three compression cycles with standard error bars. (a) Total volume change (primary plus secondary tracheae) in the tracheal regions surveyed and (b) volume change expressed as a percentage of resting (expanded) volume. (c) Volume change and (d) percentage volume change of primary and secondary tracheal branches.

wings, or legs change the volume of tracheal air sacs in a rhythmic pumping mechanism (54, 61–64, 71) that is generally in synchrony with locomotor motion. Real-time synchrotron X-ray video reveals some of the internal features of these respiratory behaviors. Grasshoppers (*Scistocerca americana*) have long, complex air sacs along the abdomen; these air sacs are synchronously compressed and expanded by abdominal motions that are known to generate gas exchange (68). Bumblebees (*Bombus*), in contrast, have large abdominal air sacs that are compressed and expanded by telescoping anteroposterior abdominal compressions (Figure 8). The air

sacs typically compress to 25–50% of expanded volume. Flight in *Drosophila* is associated with an unusual form of autoventilation in which the proboscis is protruded at regular intervals during flight, producing rapid bouts of CO<sub>2</sub> exchange that are correlated with each protrusion cycle (72). Synchrotron X-ray imaging has enabled real-time visualization of the anatomical basis of this gas exchange mechanism in a tethered fly (Figure 8) at rest: Protrusion of the proboscis results in a rapid expansion of the air sacs of the head, followed by compression of the air sacs during retraction of the proboscis (64). These results show that, even in small insects such as

**Proboscis:** the slender, tubular feeding and sucking organ of certain invertebrates, such as insects

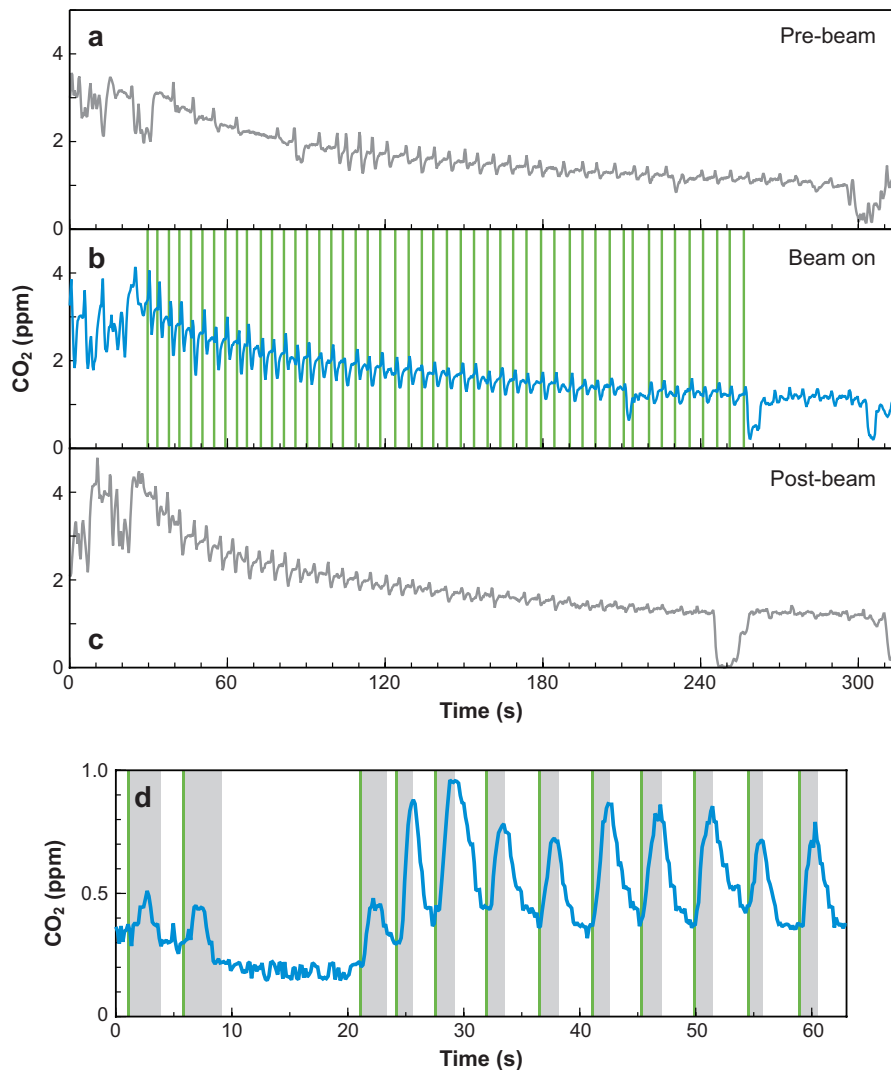


**Figure 7**

Correlation of tracheal compressions with respiratory pulses of CO<sub>2</sub> in the carabid beetle *Pterostichus stygicus* (66). (a) Respiratory CO<sub>2</sub> emission before X-ray exposure. (b) Respiratory CO<sub>2</sub> emission during X-ray exposure. Tall vertical lines (green) indicate the start of a tracheal compression, as quantified through the use of X-ray video records. (c) Respiratory CO<sub>2</sub> emission after X-ray exposure. (d) Expanded view of the relative timing of tracheal compressions and CO<sub>2</sub> pulses. In a compression cycle, a tracheal tube is compressed, held at a minimum volume, and reinflated. Green lines represent the duration of compression, and gray banding represents the total duration of the compression cycle (from compression to re-inflation). For each CO<sub>2</sub> pulse, the rise in CO<sub>2</sub> occurs simultaneously with the start of tracheal compression.

flies previously thought to rely on diffusion alone, the role of convective exchange via autoventilatory mechanisms may be significant to the respiratory physiology of structures in the head such as muscles, nervous system, and sense organs.

The role of the tracheal system and the importance of convection increase with body size in several groups of active insects (68). The use of convection allows larger insects to overcome potential diffusive limitations on oxygen delivery (73–75). Two recent studies

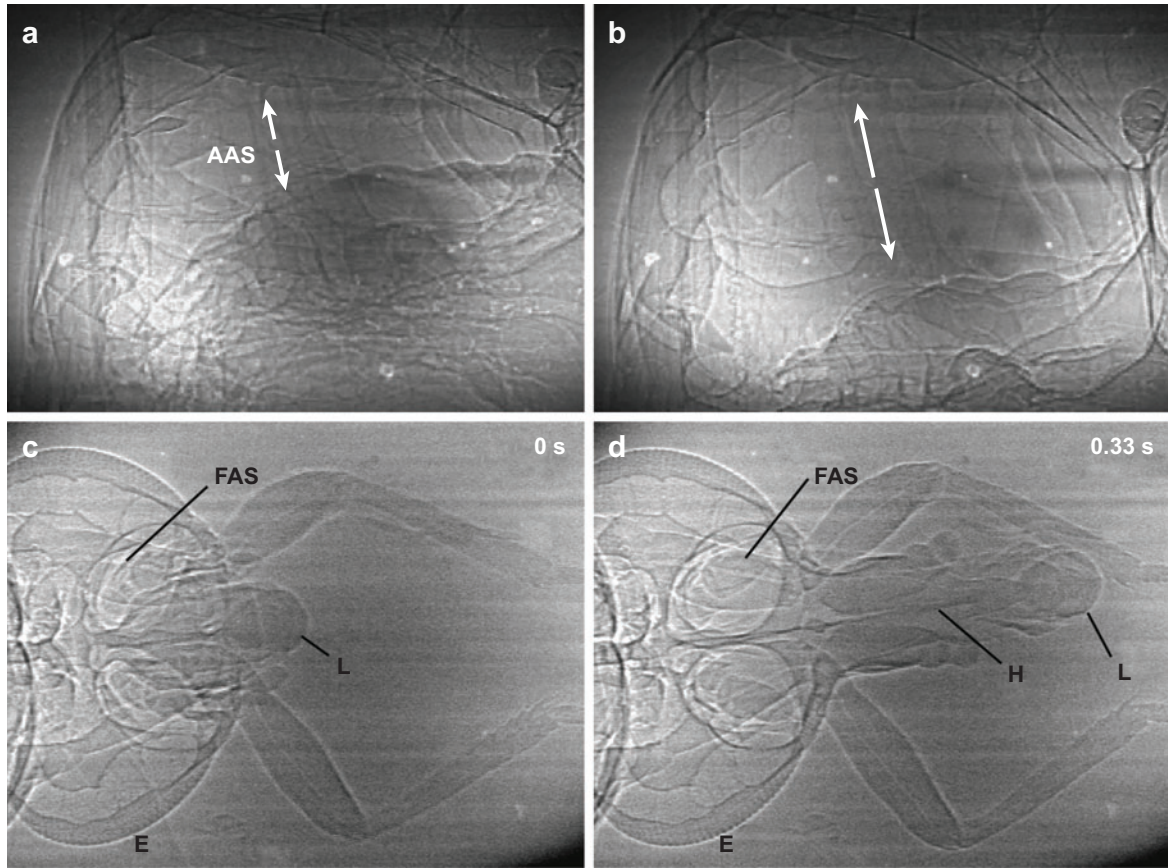


**Figure 8**

Air sac compressions in (a,b) the abdomen of a bumblebee (*Bombus*) and (c,d) the head of a fruit fly (*Drosophila*). (a) The anterior abdomen of the bumblebee showing the abdominal air sac (AAS) in the compressed position, with arrows indicating the anteroposterior air sac cavity. (b) The same air sac 0.5 s later, showing the air sac in an expanded position. (c) The frontal air sac (FAS) of a fruit fly in compressed position with the labium (L) of the proboscis in retracted position. (d) The protruded position in which the haustellum (H) and labium (L) are protruded, expanding the frontal air sac volume. E denotes the eye of the fly. Bumblebee images by M. Westneat; fruit fly images courtesy of M. Hale.

have examined the prediction that tracheal branching and total tracheal volume are positively allometric with body size (75, 76). To test this, synchrotron X-ray imaging was used to measure the relative structural and functional changes in the tracheal system during development in grasshoppers (*S. americana*) that varied in body mass from 10 mg first instars to 2 g adults (75); a similar interspecific study was done with a size series of beetles of the family Tenebrionidae (76). In grasshoppers, the volume of tracheae and especially

of air sacs in the abdomen increased strongly with body size, and the greater tidal volumes measured in larger grasshoppers (68, 75) were achieved by devoting more of their body content to compressible tracheal structures. A similar trend was found in tenebrionid beetles (76), in which larger species and individuals devoted a greater fraction of their body to the respiratory system; tracheal volume scaled positively allometrically with mass. The trends differed locally within the body: The cross-sectional area of the trachea penetrating

the leg orifice scaled strongly allometrically with mass, whereas the cross-sectional area of the head tracheae scaled isometrically with mass, suggesting that ultimately the legs may limit gas exchange. These studies suggest that insects may be able to escape size limitations imposed by diffusion by increasing tracheal volume and convection and that the space available for tracheae may ultimately limit the maximum size of some insect lineages such as beetles.

The physiology and biomechanics of insect gas exchange and the internal behavioral features of respiration are areas in which synchrotron X-ray imaging will continue to make an important contribution. The relatively novel ability to see the movements and processes inside small living animals such as insects continues to provide frequent new discoveries regarding the respiratory pattern, frequency, and biomechanics of tracheal motion. The integration of these new imaging tools with physiological instrumentation for detecting gas exchange is just beginning and promises to clarify the role of convective mechanisms in insect respiratory physiology. Major frontiers for future work remain. These include the recording of high-speed behaviors such as autoventilation during flight; the visualization of slow, sensitive resting respiratory phenomena such as the discontinuous gas exchange cycle; and the exploration of the diversity of respiratory systems in insects via synchrotron X-ray imaging in a comparative and phylogenetic context.

### Feeding Mechanisms and Mouthpart Function in Insects

Feeding mechanisms of insects provide great potential for the study of the mechanics and control of a complex functional system. However, experimental study on mouthpart feeding coordination, kinematics, and biomechanics in insects has been challenging. For example, it has not been possible to record the motions of many mouthparts because of their overlapping and often internal positions

(77, 78). Insect mouthparts are highly integrated functional systems of multiple moving appendages, which reflect the vast variety of potential food sources (79–82). One can discern several general categories of mouthparts, associated with feeding mechanisms ranging from biting and chewing on plant or animal tissue to sucking liquids with a proboscis, and intermediate forms that pierce and suck or that chew and lap. Biting and chewing insect mouthparts have paired mandibles powered by mandibular adductor and abductor muscles (51, 82) and paired maxillae composed of 3–4 movable segments controlled by up to eight muscles. The dorsal unpaired labrum and ventral multisegmented labium form the upper and lower “lips,” exerting force on a food item in opposition to other mouthparts.

Insects with sucking mouthparts include those with modified structures that allow sponging of fluids and those that pierce tissues and draw fluid into an extended proboscis (83–85). For example, feeding in specialized flies involves a proboscis formed by a modified labium that is used to pump salivary secretions onto the food item. After the item is dissolved, the fluid or suspended food is then sponged up by the pseudotracheae on the labella and is drawn into the pharynx (86). The proboscis in mosquitoes and biting flies, as well as that of hemipterans, has needle-like mouthparts for piercing and sucking. In many flies as well as most moths and butterflies, the mouthparts do not pierce the host but are used only for sucking or sponging the food (83).

Synchrotron X-ray imaging has recently been used to analyze the feeding motions and internal processing of food in several insects (14, 87), providing a unique perspective on the mechanics of both chewing and sucking mouthparts. Because food is of similar density to the animal’s soft tissue, it is necessary to introduce a marker to visualize food movement. To record X-ray video during feeding, beetles (*Pterostichus stygicus*) were fed macerated insects mixed with fine particles of cadmium powder ( $\text{CdWO}_4$ ), and butterflies (*Pieris rapae*) were fed sugar solutions laced with an

---

**Labrum:** the upper lip of insects, lying just below the clypeus on the front of the head

**Labium:** the lower lip of insects, composed of a broad shovel-like plate and fingerlike palps

**Labellum:** liplike mouthpart forming the tip of the proboscis of various insects

---

---

**Contrast agent:** a substance that produces a change in X-ray absorption in an area of interest so that it appears either darker or lighter

---

iodine contrast agent (14). The fine particles of  $\text{CdWO}_4$  had a significantly higher absorption than the beetle's soft tissue and appeared dark and granular, readily enabling particle tracking. The iodine-laced sugar solution was used in conjunction with a specific X-ray energy to maximize contrast between the food and the surrounding anatomy, rendering the food black in the X-ray.

The grasping and chewing motions of ground beetles are composed of rhythmic opening and closing of the mandibles, accompanied by coordinated rotational sweeping of the maxillae and anteroposterior motions of the labium and labial palps. Real-time synchrotron X-ray imaging provides simultaneous views of many of these motions that are difficult or impossible to obtain through conventional video. For example, we and our colleagues have achieved clear visualization of the rotational kinematics of the interior of the mandibular hinge joints, the rotational action of the bases of the maxillae, the anteroposterior motion of the labium as food is drawn into the mouth, and the patterns of autoventilatory compression of the tracheae that run through the jaw muscles (65).

Relatively little is known about the internal dynamics of liquid transport in insects during feeding. Synchrotron X-ray imaging has been a key to understanding how butterflies suck food through the proboscis and transport food within the head (87). X-ray video was recorded while butterflies (*P. rapae*) ingested a sugar water/iodine mixture (**Figure 9**), enabling visualization of the sucking pump and transport in the esophagus. Butterflies ingested food, using a two-phase process, intake and ejection (**Figure 9**). The ingestion and transport mechanism of ants during liquid feeding were also recently explored through the use of real-time synchrotron X-ray imaging (**Figure 9**). This research led to the discovery of a multi-phase process in which the glossa and cibarium draw fluids into the mouth, boluses of fluid are pumped to a repository located in the anterior esophagus, and these boluses are then transported along the length of the esopha-

gus to the crop (**Figure 9**). This work helps explain the mechanics of how some ants use rapid feeding in their roles as highly successful exploitative competitors of liquid resources. The ant and butterfly studies demonstrate the effectiveness of synchrotron X-ray imaging in combination with labeling agents for food tracking in small organisms and highlight promising avenues of research for the exploration of the ingestion and digestion processes of insects with a diversity of feeding mechanisms.

### Functional Imaging in Vertebrate Systems

Synchrotron imaging has been used in a wide variety of medical imaging applications, including coronary angiography in human patients (88, 89), and in both clinical practice and animal model studies (90–95). Although applications of phase imaging have not been as frequently applied to comparative vertebrate physiology and function, there are several published studies of lung and brain function in living but anesthetized mammals, and some synchrotron imaging data exist for small living fishes. A series of recent studies (96–98) has used rat and rabbit lung preparations, either excised lungs or anesthetized animals, to visualize respiratory function in mammals. Using mechanically ventilated rabbits and inhaled xenon gas, recent research (96, 97) used synchrotron imaging to generate high-resolution maps of air flow and changes in pulmonary gas distribution in the lungs. A second research group (98) has provided insight into the biomechanical properties of small airways in lung tissue by visualizing changes in tissue morphology during ventilation. Several particularly compelling examples of imaging of lung function are the recent comparative lung imaging of mice and rabbits (99) and a developmental study of neonate lung function in rabbits (100), in which the first clearing of the lungs after birth and initial sites of airway inflation were revealed. Also in the rat model, through the use of contrast agents

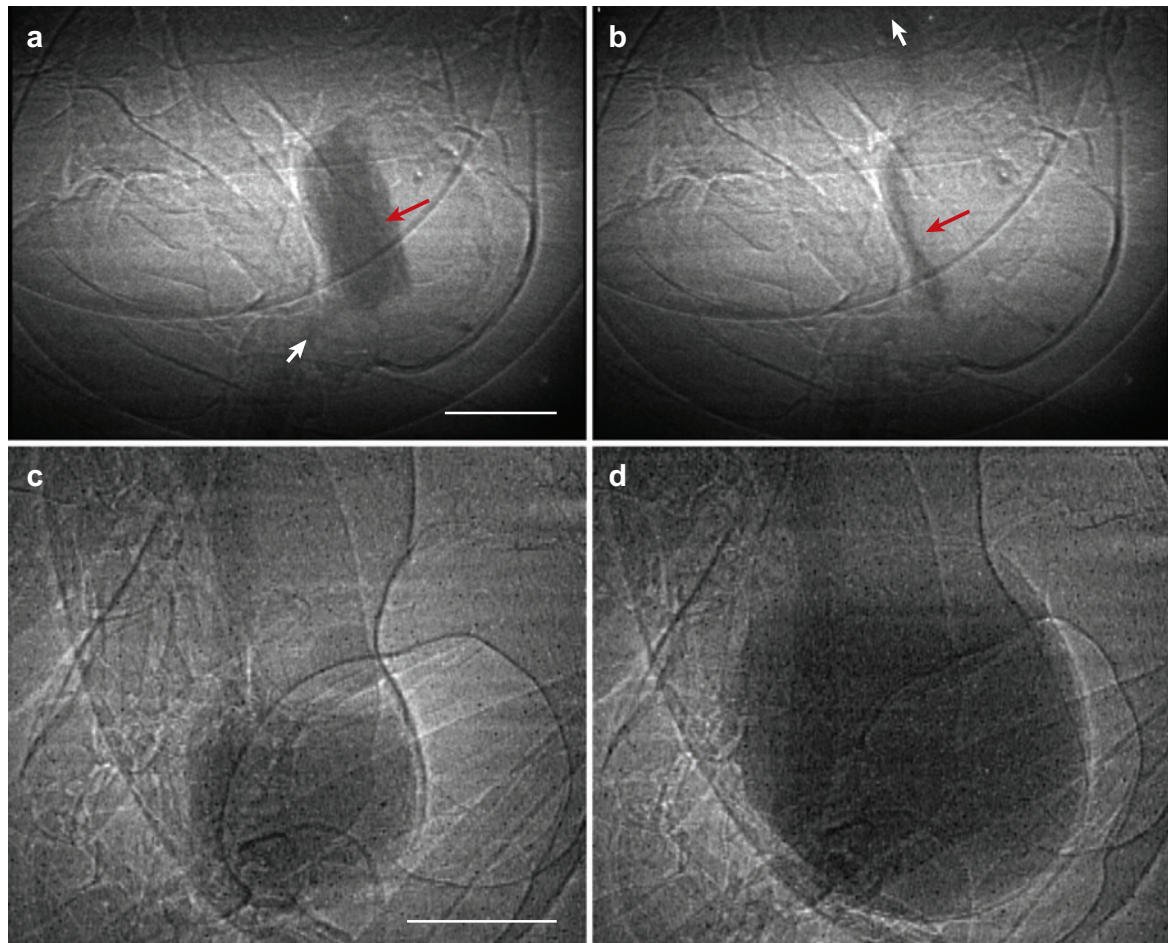


**Figure 9**

X-ray images of fluid transport in butterfly and ant feeding. The ingestion processes of liquid feeding were visualized using a K-edge contrast agent. Iodine was used as a contrast agent, with X-rays (33.25 keV) tuned just above the iodine K-edge to increase absorption. (a) Lateral view of head of a butterfly, *Pieris rapae*, during food intake effected by the sucking pump (87). Anterior is down, and posterior is up. As the roof of the buccal chamber is pulled dorsally (red arrow), food is pumped through the proboscis (not shown) and cibarium (white arrow) into the buccal chamber. (b) During ejection, the roof of the buccal chamber is pushed ventrally (red arrow), forcing food posteriorly into the esophagus (white arrow). (c,d) Lateral view of the anterior abdomen of an ant, *Camponotus herculeanus*, showing the filling of the crop during feeding (images courtesy of S. Cook). Time interval between frames is 42 s. Scale bars, 250  $\mu$ m.

to track blood flow in anesthetized animals, synchrotron imaging was used (101) to create cerebral blood flow maps with a higher resolution than standard MRI techniques. Finally, current research is expanding the application of synchrotron imaging to other vertebrate systems such as fishes. **Figure 10** illustrates the pharyngeal and oral jaws in a living, lightly

anesthetized cichlid fish during respiratory cycles. The contrast of the images is attenuated somewhat by the X-ray beam passing through a layer of water around the fish, but the internal mobility of the pharyngeal jaws and hyoid is clearly visible, contributing to our understanding of internal motion in complex vertebrate skulls.

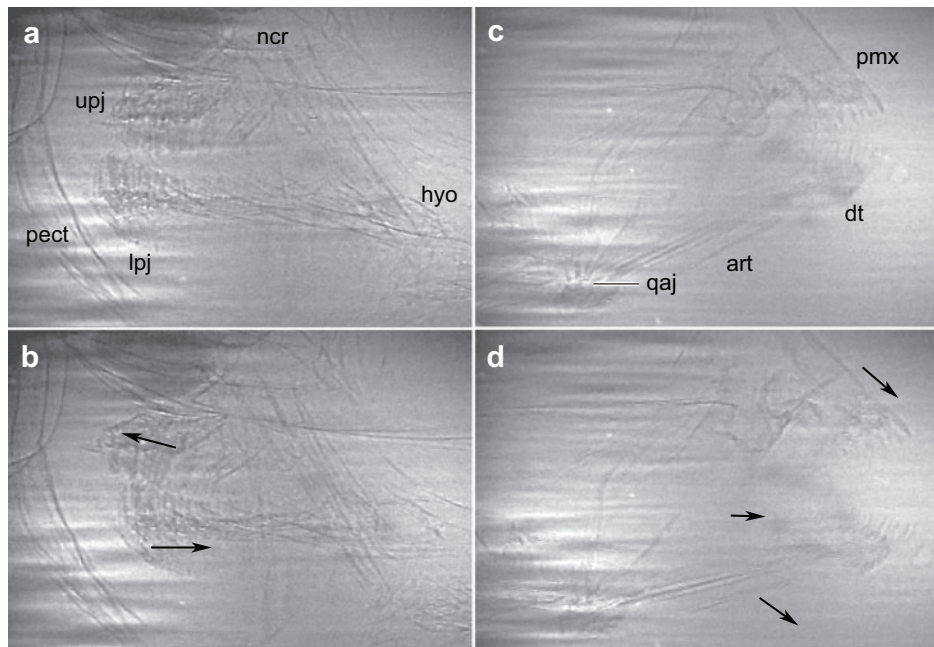


**Figure 10**

Frames from a real-time synchrotron X-ray video of the head of a small cichlid fish (*Geophagus* sp.) during pharyngeal jaw manipulation and respiration, recorded with the X-rays passing through water as well as the living specimen. (a) Upper (upj) and lower (lpj) pharyngeal jaws. Also visible are the ventral neurocranium (ncr), pectoral girdle (pect), and hyoid (hyo) (anterior to the *right*). (b) The lower jaw is pulled anteriorly, and the upper jaw is rotated posterodorsally to bring the pharyngeal jaws together in a sliding pharyngeal bite. Arrows indicate jaw motions. (c,d) Anterior jaws of the same specimen, including the premaxilla (pmx), dentary (dt), articular (art), and quadrate-articular joint (qaj), in (c) a relatively retracted position and (d) a protruded position in which the lower jaw rotates ventrally and the premaxilla protrudes. Arrows indicate jaw motions. Images courtesy of M. Hale and M. Westneat.

### Imaging and Radiation Impact Trade-Offs in Live Animal Synchrotron Imaging

A recent experimental paper (14) examined the effects of synchrotron radiation on animal behavior and physiological condition and showed the importance of assessing the effects of X-rays on the animal when using X-rays to study physiological processes. In general, X-ray imaging involves a trade-off between image quality and survivorship: Higher-quality images require greater exposures to radiation, which result in greater harm to the animal. By varying X-ray parameters and using CO<sub>2</sub> emission patterns and motor behaviors to assess physiological damage in four

insect species, this work was able to determine a combination of X-ray beam parameters that maximized image quality while minimizing damage to the animal, which depends on dose (102). The literature (103–105) suggests that for full-body irradiation, there are no observable physiological effects at doses of less than 500 Gy, a temporary loss of motor control is observed after ~1.5 kGy, and a more permanent loss of motor control occurs at doses greater than 2.5 kGy. The central conclusion of this study (14) was that current third-generation synchrotron sources are capable of visualizing naturalistic behaviors and processes in insects for minutes and longer at the millimeter scale with micron resolution. Furthermore, insects do not heat in the beam.

In general, for insect physiology and behavior there was a satisfactory compromise between image quality and survivorship by the use of 25 keV X-rays at 80 mW mm<sup>-2</sup> flux density ( $2 \times 10^{10}$  ph s<sup>-1</sup> mm<sup>-2</sup>) and 1 m sample-detector distance. The duration of time that an insect can be visualized is a function of both X-ray parameters and the location of X-rays on the body.

However, because of the many factors that bear on the question of image quality vs survivorship, no single set of X-ray parameters provides an optimal setting. Generally, one would like (a) a very small synchrotron source size to minimize image blur and (b) an efficient detector system so that a less intense X-ray beam can be used to maximize survivorship. In practice, for animal physiology, the first question is whether a desired internal dynamic or morphology can be visualized by this technique. Given a particular synchrotron source and detector system, one usually starts with parameters that give superior image quality. On the basis of our experience with insects, this is usually with an X-ray energy of 10–20 keV and a sample-detector distance of 10–100 cm. After the desired feature is visualized, the system can be optimized on the basis of the relative importance of image contrast, spatial resolution, and survivorship.

## CONCLUSIONS

Synchrotron X-ray imaging provides a fascinating new window into the internal structure and function of small organisms that is revolutionizing multiple areas of biological and medical research. The power and application of this technique in the area of CT are already well established, with numerous examples of 3-D reconstruction for morphology, developmental biology, and paleontology. Another important area of physiological research, not a focus of this review, is the use of synchrotron radiation for diffraction studies of muscle function (106–108), which have greatly clarified the actin-myosin muscle motor system. For living animal physiol-

ogy, synchrotron X-ray imaging has just begun to be applied to a wide range of problems such as respiration, feeding, and internal transport mechanisms. Synchrotron X-ray phase-contrast imaging is the only available technique that has the spatial and temporal resolution, penetrating power, and sensitivity to soft tissue that is required to visualize the internal physiology of small living animals on a scale from millimeters to microns. Synchrotron X-ray imaging of live animals either is having a major impact or is poised to make a strong contribution to physiology in multiple areas. The first is the biomechanical mechanisms of tracheal compression and the role of convective respiratory mechanisms in insect physiology and evolution (13, 75, 76). Diverse respiratory mechanisms in insects, from rapid autoventilation of air sacs during flight to slower discontinuous respiratory cycles, will be more comprehensible with a clear internal view of respiratory system behavior. Another promising area of research is the visualization of complex circulatory patterns within insects, including hemolymph transport and the function of pulsatile organs. Preliminary observations reveal that pulsatile organs and circulatory pumps are visible during contractions, but techniques of increasing the contrast of circulatory fluids would greatly aid the visualization of internal fluid motions in small animals. Another area of increasing research activity is the feeding mechanisms of insects, focused on the rapidly moving internal mouthparts of biting insects and the visualization of fluid motion in the pumping organs of fluid-feeding insects such as flies and butterflies. More broadly, the synchrotron X-ray window into internal function is likely to show us previously unknown functional traits of mouthparts, pharyngeal pumps, digestive systems, leg joints, and wing mechanisms in insects, other arthropods, and small vertebrates. The first synchrotron research on living vertebrate musculoskeletal systems has recently begun with medical imaging of lung function in rabbit and rat preparations as well as successful real-time X-ray video of the interior

bones of the pharynx and skull during fish respiration. The development of highly light-sensitive high-speed video systems is also now being used to record fast motions such as flight and feeding in the X-ray beam. Finally, recent work on fruit fly respiration and feeding (64) illustrates the impact of X-ray imaging research in model systems such as fly, zebrafish, and mouse, in which the mechanisms of heart,

circulatory, digestive, and locomotor systems can be analyzed in new ways and compared with those of mutants or disease models that may be used to study human health concerns. Through these research directions and others, synchrotron X-ray imaging will continue to make important contributions to our understanding of organismal structure, physiology, and evolution.

### SUMMARY POINTS

1. Synchrotron X-ray imaging is a new, high-resolution approach to microscopy that can perform nondestructive still imaging and real-time X-ray video of internal function in small organisms.
2. The method of synchrotron X-ray imaging, including recommendations for use of the method with live animals in physiological experiments, is explained.
3. Computed tomography using synchrotron imaging has made a major impact on 3-D reconstruction of complex morphology in small organisms ranging from seeds to sponges to beetles to fossil embryos.
4. The functional morphology and physiology of insect respiration have been greatly advanced through the use of phase-enhanced X-ray imaging in beetles, ants, flies, and a wide range of other insects.
5. The feeding mechanisms of chewing and sucking insects have been studied via X-ray imaging, with an important contribution to the tracking of food and fluid transport inside the animals through the use of contrast agents added to the food.
6. Vertebrate respiration and skull mechanisms have also been studied, through synchrotron X-ray imaging, in mammals such as rat and rabbit lung preparations as well as small fishes.
7. Synchrotron X-ray imaging provides an exciting new window into the internal workings of small animals. This technique has future promise to contribute to a range of physiological and biomechanical questions in comparative biology.

### DISCLOSURE STATEMENT

The authors are not aware of any biases that might be perceived as affecting the objectivity of this review.

### ACKNOWLEDGMENTS

Thanks to the many collaborators who contributed to the insect physiology sections of this paper, including O. Betz, K. Fezzaa, J. Harrison, M. Hale, and J. Waters. Portions of this research were funded by NSF 0235307 to M. Westneat. Use of the Advanced Photon Source was supported by the U.S. Department of Energy, Office of Science, Office of Basic Energy Sciences, under Contract No. DE-AC02-06CH11357.

## LITERATURE CITED

1. Murphy DB. 2001. *Fundamentals of Light Microscopy and Electronic Imaging*. New York: Wiley-Liss
2. Michalet X, Kapanidis AN, Laurence T, Pinaud F, Doose S, et al. 2003. The power and prospects of fluorescence microscopies and spectroscopies. *Annu. Rev. Biophys. Biomol. Struct.* 32:161–82
3. Kalender W. 2006. Review: X-ray computed tomography. *Phys. Med. Biol.* 51:R29–43
4. Lauder GV, Madden PGA. 2008. Advances in comparative physiology from high-speed imaging of animal and fluid motion. *Annu. Rev. Physiol.* 70:143–63
5. Snigirev A, Snigireva I, Kohn V, Kuznetsov S, Schelokov I. 1995. On the possibilities of x-ray phase contrast microimaging by coherent high-energy synchrotron radiation. *Rev. Sci. Instr.* 66:5486–92
6. Cloetens P, Barrett R, Baruchel J, Guigay JP, Schlenker M. 1996. Phase objects in synchrotron radiation hard x-ray imaging. *J. Phys. D* 29:133–46
7. Gatesy SM. 1999. Guineafowl hind limb function. I: Cineradiographic analysis and speed effects. *J. Morph.* 240:115–25
8. Sun Z, Liu ZJ, Herring SW. 2002. Movement of temporomandibular joint tissues during mastication and passive manipulation in miniature pigs. *Arch. Oral. Biol.* 47:293–305
9. Brainerd EL. 1999. New perspectives on the evolution of lung ventilation mechanisms in vertebrates. *Exp. Biol. Online* 4:11–28
10. Ridgway C, Chambers J. 1998. Detection of insects inside wheat kernels by NIR imaging. *J. Near Infrared Spectrosc.* 6:115–19
11. Hart AG, Bowtell RW, Kockenberger W, Wenseleers T, Ratnieks FLW. 2003. Magnetic resonance imaging in entomology: a critical review. *J. Insect Sci.* 3:1–9
12. Harris RA, Follett DH, Halliwell M, Wells PNT. 1991. Ultimate limits in ultrasonic imaging resolution. *Ultrasound Med. Biol.* 17:547–58
13. Westneat MW, Betz O, Blob RW, Fezzaa K, Cooper WJ, Lee WK. 2003. Tracheal respiration in insects visualized with synchrotron x-ray imaging. *Science* 299:558–60
14. Socha JJ, Westneat MW, Harrison JF, Waters JS, Lee W-K. 2007. Real-time phase-contrast x-ray imaging: a new technique for the study of animal form and function. *BMC Biol.* 5:6
15. Betz O, Wegst U, Weide D, Heethoff M, Helfen L, et al. 2007. Imaging applications of synchrotron x-ray microtomography in biological morphology and biomaterial science. I. General aspects of the technique and its advantages in the analysis of arthropod structure. *J. Microsc.* 227:51–71
16. Fitzgerald R. 2000. Phase-sensitive x-ray imaging. *Phys. Today* 53:23–27
17. Cloetens P, Pateyron-Salome M, Buffiere JY, Peix G, Baruchel J, et al. 1997. Observation of microstructure and damage in materials by phase sensitive radiography and tomography. *J. Appl. Phys.* 81:5878–86
18. Larabell CA, Le Gros MA. 2004. X-ray tomography generates 3-D reconstructions of the yeast, *Saccharomyces cerevisiae*, at 60-nm resolution. *Mol. Biol. Cell* 15:957–62
19. Shapiro D, Thibault P, Bietz T, Elser V, Howells M, et al. 2004. Biological imaging by soft x-ray diffraction microscopy. *Proc. Natl. Acad. Sci. USA* 102:15343–46
20. Lai B, Maser J, Vogt S, Cai Z, Legnini D. 2004. Imaging and quantifying major/trace elemental distribution. *Microsc. Microanal.* 10:1284–85
21. Beckmann F, Heise K, Kölsch B, Bonse U, Rajewsky MF, et al. 1999. Three-dimensional imaging of nerve tissue by x-ray phase-contrast microtomography. *Biophys. J.* 76:98–102

22. Cloetens P, Mache R, Schlenker M, Lerbs-Mache S. 2006. Quantitative phase tomography of *Arabidopsis* seeds reveals intercellular void network. *Proc. Natl. Acad. Sci. USA* 103:1426–30
23. Westermann B, Ruth P, Litzlebauer HD, Beck I, Beuerlein K, et al. 2002. The digestive tract of *Nautilus pompilius* (Cephalopoda, Tetrabranchiata): an X-ray analytical and computational tomography study on the living animal. *J. Exp. Biol.* 205:1617–24
24. Bonse U, Busch F. 1996. X-ray computed microtomography ( $\mu$ CT) using synchrotron radiation (SR). *Prog. Biophys. Mol. Biol.* 65:133–69
25. Itai Y, Takeda T, Akatsuka T, Maeda T, Hyodo K, et al. 1995. High contrast computed tomography with synchrotron radiation. *Rev. Sci. Instrum.* 66:1385–87
26. Kinney JH, Nichols MC. 1992. X-ray tomographic microscopy (XTM) using synchrotron radiation. *Annu. Rev. Mater. Sci.* 22:121–52
27. Smith JV. 1995. Synchrotron X-ray sources: instrumental characteristics, new applications in microanalysis, tomography, absorption spectroscopy and diffraction. *Analyst* 120:1231–45
28. Suortti P, Thomlinson W. 2003. Medical applications of synchrotron radiation. *Phys. Med. Biol.* 48:R1–35
29. Ritman EL. 2004. Micro-computed tomography: current status and developments. *Annu. Rev. Biomed. Eng.* 6:185–208
30. Cloetens P, Boller E, Ludwig W, Baruchel J, Schlenker M. 2001. Absorption and phase imaging with synchrotron radiation. *Europhys. News* 32:1–9
31. Maire E, Buffière J-Y, Salvo L, Blandin JJ, Ludwig W, Létang JM. 2001. On the application of X-ray microtomography in the field of materials science. *Adv. Eng. Mater.* 3:539–46
32. Mayo SC, Davis TJ, Gureyev TE, Miller PR, Paganin D, et al. 2003. X-ray phase-contrast microscopy and microtomography. *Optics Express* 11:2289–302
33. Nickel M, Donath T, Schweikert M, Beckmann F. 2006. Functional morphology of *Tethya* species (Porifera): 1. Quantitative 3D-analysis of *T. wilhelma* by synchrotron radiation based x-ray microtomography. *Zoomorphology* 125:209–23
34. Kim SA, Punshon A, Lanzirotti A, Li L, Alonso JM, et al. 2006. Localization of iron in *Arabidopsis* seed requires the vacuolar membrane transporter VIT1. *Science* 314:1295–98
35. McNear DH, Peltier E, Everhart J, Chaney RL, Sutton S, et al. 2005. Application of quantitative fluorescence and absorption-edge computed microtomography to image metal compartmentalization in *Alyssum murale*. *Environ. Sci. Technol.* 39:2210–18
36. Young LW, Westcott ND, Attenkofer K, Reaney MJ. 2006. A high-throughput determination of metal concentrations in whole intact *Arabidopsis thaliana* seeds using synchrotron-based X-ray fluorescence spectroscopy. *J. Synchrotron Radiat.* 13:304–13
37. DeVore ML, Kenrick P, Pigg KB, Ketcham RA. 2006. Utility of high resolution x-ray computed tomography (HRXCT) for paleobotanical studies: an example using London Clay fruits and seeds. *Am. J. Bot.* 93:1848–51
38. Braiden AK, Orr PJ, Tafforeau P. 2006. X-ray synchrotron microtomographic imaging of three-dimensional non-biomineralized fossil arthropods from upper Triassic shoreface clays, Somerset, England. *Geophys. Res. Abstr.* 8:11038–39
39. Tafforeau P, Boistel R, Boller E, Bravin A, Brunet M, et al. 2006. Applications of X-ray synchrotron microtomography for nondestructive 3D studies of paleontological specimens. *Appl. Phys. A* 83:195–202
40. Mazurier A, Volpato V, Macchiarelli R. 2006. Improved noninvasive microstructural analysis of fossil tissues by means of SR-microtomography. *Appl. Phys. A* 83:229–33

41. Donoghue PCJ, Bengtson S, Dong X-P, Gostling NJ, Hultgren T, Cunningham JA. 2006. Synchrotron X-ray tomographic microscopy of fossil embryos. *Nature* 442:680–83
42. Chen J-Y, Bottjer DJ, Davidson EH, Dornbos SQ, Gao X, et al. 2006. Phosphatized polar lobe-forming embryos from the Precambrian of Southwest China. *Science* 312:1644–46
43. Stock SR, Barss J, Dahl T, Veis A, Almer JD, De Carlo F. 2003. Synchrotron x-ray studies of the keel of the short-spined sea urchin *Lytechinus variegatus*: absorption microtomography (microCT) and small beam diffraction mapping. *Calcif. Tissue Int.* 72:555–66
44. Stock SR, Ignatiev K, Dahl T, Barss J, Fezzaa K, et al. 2003. Multiple microscopy modalities applied to a sea urchin tooth fragment. *J. Synchrotron Radiat.* 10:393–97
45. Wirkner CS, Richter S. 2004. Improvement of microanatomical research by combining corrosion casts with MicroCT and 3D reconstruction, exemplified in the circulatory organs of the woodlouse. *Microsc. Res. Tech.* 64:250–54
46. Prymak O, Tiemann H, Sötje I, Marxen JC, Klocke A, et al. 2005. Application of synchrotron-radiation-based computer microtomography (SR  $\mu$  CT) to selected biominerals: embryonic snails, statoliths of medusae, and human teeth. *J. Biol. Inorg. Chem.* 10:688–95
47. Postnov A, DeClerck N, Sasov A, VanDyck D. 2002. 3D in-vivo X-ray microtomography of living snails. *J. Microsc.* 205:201–4
48. Van Spaendonck MP, Cryns K, Van de Heyning PH, Scheuermann DW, Van Camp G, Timmermans J-P. 2000. High resolution imaging of the mouse inner ear by microtomography: a new tool in inner ear research. *Anat. Rec.* 259:229–36
49. Beckmann F, Heise K, Kölsch B, Bonse U, Rajewsky MF, et al. 1999. Three-dimensional imaging of nerve tissue by x-ray phase-contrast microtomography. *Biophys. J.* 76:98–102
50. Plouraboué F, Cloetens P, Fonta C, Steyer A, Lauwers F, Marc-Vergnes J-P. 2004. X-ray high-resolution vascular network imaging. *J. Microsc.* 215a:139–48
51. Chapman RF. 1998. *The Insects: Structure and Function*. Cambridge, UK: Cambridge Univ. Press. 4th ed.
52. Lighton JRB, Fukushi T, Wehner R. 1993. Ventilation in *Cataglyphis bicolor*: regulation of carbon dioxide release from the thoracic and abdominal spiracles. *J. Insect Physiol.* 39:687–99
53. Mill PJ. 1985. Structure and physiology of the respiratory system. In *Comprehensive Insect Physiology*, ed. GA Kerkut, LJ Gilbert, pp. 517–93. Oxford: Pergamon
54. Miller PL. 1960. Respiration in the desert locust: III. Ventilation and the spiracles during flight. *J. Exp. Biol.* 37:264–78
55. Kestler P. 1985. Respiration and respiratory water loss. In *Environmental Physiology and Biochemistry of Insects*, ed. KH Hoffmann, pp. 137–83. Berlin: Springer-Verlag
56. Krogh A. 1920. Studien über Tracheenrespiration. II. Über die Gasdiffusion in den Tracheen. *Pflügers Arch.* 179:95–112
57. Loudon C. 1989. Tracheal hypertrophy in mealworms: design and plasticity in oxygen supply systems. *J. Exp. Biol.* 147:217–36
58. Chown SL, Davis ALV. 2003. Discontinuous gas exchange and the significance of respiratory water loss in scarabaeine beetles. *J. Exp. Biol.* 206:3547–56
59. Levy RI, Schneiderman HA. 1966. Discontinuous respiration in insects. II. The direct measurement and significance of changes in tracheal gas composition during the respiratory cycle of silkworm pupae. *J. Insect Physiol.* 12:83–104
60. Lighton JRB. 1996. Discontinuous gas exchange in insects. *Annu. Rev. Entomol.* 141:309–24
61. Miller PL. 1981. Ventilation in active and inactive insects. In *Locomotion and Energetics in Arthropods*, ed. CF Herreid, CR Fournier, pp. 367–90. New York: Plenum

62. Wasserthal LT. 2001. Flight-motor driven respiratory air flow in the hawkmoth *Manduca sexta*. *J. Exp. Biol.* 204:2209–20
63. Weis-Fogh T. 1967. Respiration and tracheal ventilation in locusts and other flying insects. *J. Exp. Biol.* 47:561–87
64. Hale ME, Waters JS, Lee W-K, Socha JJ, Fezzaa K, Westneat MW. 2007. Drawing inspiration from insect breathing and heaving conventional wisdom: convective tracheal and air sac mechanisms in *Drosophila* visualized with x-ray imaging. *Int. Comp. Biol.* 46:133
65. Westneat MW, Socha JJ, Betz O, Fezzaa K, Lee W-K. 2007. Tracheal compression mechanisms in the beetle *Platynus decentis* (Carabidae) visualized with synchrotron x-ray imaging. *J. Insect Physiol.* In review
66. Socha JJ, Lee W-K, Harrison JF, Westneat MW. 2005. Tubes squeeze and the air flows out: correlated patterns of CO<sub>2</sub> emission and tracheal compression in the beetle *Platynus decentis* (Carabidae). *Int. Comp. Biol.* 45:1074
67. Harrison JF. 1997. Ventilatory mechanism and control in grasshoppers. *Am. Zool.* 37:73–81
68. Greenlee KJ, Harrison JF. 2004. Development of respiratory function in the American locust *Schistocerca americana*. I. Across instar effects. *J. Exp. Biol.* 207:497–508
69. Wasserthal LT. 1976. Heartbeat reversal and its coordination with accessory pulsatile organs and abdominal movements in Lepidoptera. *Experientia* 32:577–79
70. Kuusik A, Johannes M, Mand M, Metspalu L, Tartes U, Lind A. 2004. Cyclic release of carbon dioxide accompanied by abdominal telescoping movements in forager ants of *Formica polyctena* (Hymenoptera, Formicidae). *Physiol. Entomol.* 29:152–58
71. Weis-Fogh T. 1967. Respiration and tracheal ventilation in locusts and other flying insects. *J. Exp. Biol.* 47:561–87
72. Lehmann F-O, Heymann N. 2005. Unconventional mechanisms control cyclic respiratory gas release in flying *Drosophila*. *J. Exp. Biol.* 208:3645–54
73. Harrison JF, LaFreniere JJ, Greenlee KJ. 2005. Ontogeny of tracheal dimensions and gas exchange capacities in the grasshopper, *Schistocerca americana*. *Comp. Biochem. Physiol. A* 141:372–80
74. Hartung DK, Kirkton SD, Harrison JF. 2004. Ontogeny of tracheal system structure: a light and electron-microscopic study of the metathoracic femur of the American locust, *Schistocerca americana*. *J. Morphol.* 262:800–12
75. Harrison JF, Greenlee KJ, Henry JR, Kirkton SD, Westneat MW, et al. 2007. Tracheal hyperallometry explains oxygen limits on insect size. *Proc. R. Soc. London Ser. B*. In review
76. Kaiser A, Klok CJ, Socha JJ, Lee W-K, Quinlan MC, Harrison JF. 2007. Increase in tracheal investment with beetle size supports hypothesis of oxygen limitation on insect gigantism. *Proc. Natl. Acad. Sci. USA* 104:13198–203
77. Evans MEG, Forsythe TG. 1985. Feeding mechanisms, and their variation in form, of some adult ground beetles (Coleoptera: Caraboidea). *J. Zool. London A* 206:113–43
78. Borrell BJ. 2003. Suction feeding in orchid bees (Apidae: Euglossini). *Proc. R. Soc. London Ser. B* 271(Suppl. 4):164–66
79. Krenn HW, Plant JD, Szucsich NU. 2005. Mouthparts of flower-visiting insects. *Arth. Struct. Dev.* 34:1–40
80. Betz O, Thayer MK, Newton AF. 2003. Comparative morphology and evolutionary pathways of the mouthparts in spore-feeding Staphylinoida (Coleoptera). *Acta Zool.* 84:179–238
81. Labandeira CC. 1997. Insect mouthparts: ascertaining the paleobiology of insect feeding strategies. *Annu. Rev. Ecol. Syst.* 28:153–93

82. Smith JJB. 1985. Feeding mechanisms. In *Comprehensive Insect Physiology, Biochemistry and Pharmacology*, Vol. 4, ed. GA Kerkut, LI Gilbert, pp. 33–85. Oxford, UK: Pergamon
83. Daniel TL, Kingsolver JG, Meyhoefer E. 1989. Mechanical determinants of nectar-feeding energetics in butterflies: muscle mechanics, feeding geometry, and functional equivalence. *Oecologia* 79:66–75
84. Krenn HW. 1990. Functional morphology and movements of the proboscis of Lepidoptera (Insecta). *Zoomorphol.* 110:105–14
85. Vijaysegaran S, Walter GH, Drew RAI. 1997. Mouthpart structure, feeding mechanisms and natural food sources of adult Bactrocera (Diptera: Tephritidae). *Ann. Entomol. Soc. Am.* 90:184–201
86. Van der Starre H, Ruigrok T. 1980. Proboscis extension and retraction in the blowfly *Calliphora vicina*. *Physiol. Entomol.* 5:87–92
87. Socha JJ, Waters JS, Westneat MW, LaBarbera M, Cook SC, et al. 2006. The poise that refreshes: dynamics of internal fluid transport during feeding in a butterfly. *Integ. Comp. Biol.* 46:133
88. Rubenstein E, Hofstadter R, Zeman HD, Thompson AC, Otis JN, et al. 1986. Transvenous coronary angiography in humans using synchrotron radiation. *Proc. Natl. Acad. Sci. USA* 83:9724–28
89. Bertrand B, Estève F, Elleaume H, Némóz C, Fiedler S, et al. 2005. Comparison of synchrotron radiation angiography with conventional angiography for the diagnosis of in-stent restenosis after percutaneous transluminal coronary angioplasty. *Eur. Heart J.* 26:1284–91
90. Lewis RA. 2004. Medical phase contrast x-ray imaging: current status and future prospects. *Phys. Med. Biol.* 49:3573–83
91. Ando M, Hashimoto E, Hashizume H, Hyodo K, Inoue H, et al. 2005. Clinical step onward with X-ray dark-field imaging and perspective view of medical applications of synchrotron radiation in Japan. *Nucl. Inst. Methods Phys. Res. A* 548:1–16
92. Thomlinson W, Suortti P, Chapman D. 2005. Recent advances in synchrotron radiation medical research. *Nucl. Inst. Methods Phys. Res. A* 543:288–96
93. Chou CY, Anastasio MA, Brankov JG, Wernick MN, Brey EM, et al. 2007. An extended diffraction-enhanced imaging method for implementing multiple-image radiography. *Phys. Med. Biol.* 52:1923–45
94. Liu CL, Yan XH, Zhang XY, Yang WT, Peng WJ, et al. 2007. Evaluation of x-ray diffraction enhanced imaging in the diagnosis of breast cancer. *Phys. Med. Biol.* 52: 419–27
95. Müller B, Bernhardt R, Weitkamp T, Beckmann F, Bräuer R, et al. 2007. Morphology of bony tissues and implants uncovered by high-resolution tomographic imaging. *Int. J. Mater. Res.* 98:613–21
96. Porra L, Monfraix S, Berruyer G, Le Duc G, Nemoz C, Thomlinson W, et al. 2004. Effect of tidal volume on distribution of ventilation assessed by synchrotron radiation CT in rabbit. *J. Appl. Physiol.* 96:1899–908
97. Monfraix S, Bayat S, Porra L, Berruyer G, Nemoz C, et al. 2005. Quantitative measurement of regional lung gas volume by synchrotron radiation computed tomography. *Phys. Med. Biol.* 50:1–11
98. Sera T, Fujioka H, Yokota H, Makinouchi A, Himeno R, et al. 2004. Localized compliance of small airways in excised rat lungs using microfocal X-ray computed tomography. *J. Appl. Physiol.* 96:1665–73
99. Kitchen MJ, Lewis RA, Yagi N, Uesugi K, Paganin D, et al. 2005. Phase contrast x-ray imaging of mice and rabbit lungs: a comparative study. *Br. J. Radiol.* 78:1018–27

100. Lewis RA, Yagi N, Kitchen MJ, Morgan MJ, Paganin D, et al. 2005. Dynamic imaging of the lungs using x-ray phase contrast. *Phys. Med. Biol.* 50:5031–40
101. Adam J-F, Elleaume H, Le Duc G, Corde S, Charvet A-M, et al. 2003. Absolute cerebral blood volume and blood flow measurements based on synchrotron radiation quantitative computed tomography. *J. Cereb. Blood Flow Metab.* 23:499–512
102. Grosch DS. 1962. Entomological aspects of radiation as related to genetics and physiology. *Annu. Rev. Entomol.* 7:81–106
103. Megumi T, Gamo S, Ohonishi T, Tanaka Y. 1995. Induction of leg-shaking, knock-down and killing responses by gamma-ray irradiation in *Shaker* mutants of *Drosophila melanogaster*. *J. Radiat. Res.* 36:134–42
104. Grosch DS. 1956. Induced lethargy and the radiation control of insects. *J. Econ. Entomol.* 49:629–31
105. Heidenthal G. 1945. The occurrence of x-ray induced dominant lethal mutations in *Habrobracon*. *Genetics* 30:197–205
106. Dickinson M, Farman G, Frye M, Bekyarova T, Gore D, et al. 2005. Molecular dynamics of cyclically contracting insect flight muscle in vivo. *Nature* 433:330–34
107. Wakabayashi K, Tokunaga M, Kohno I. 1992. Small-angle synchrotron X-ray scattering reveals distinct shape changes of the myosin head during hydrolysis of ATP. *Science* 258:443–47
108. Irving TC, Maughan DW. 2000. In vivo x-ray diffraction of indirect flight muscle from *Drosophila melanogaster*. *Biophys. J.* 78:2511–15



# Contents

Frontispiece <i>Joseph F. Hoffman</i> .....	xvi
<b>PERSPECTIVES, David Julius, Editor</b>	
My Passion and Passages with Red Blood Cells <i>Joseph F. Hoffman</i> .....	1
<b>CARDIOVASCULAR PHYSIOLOGY, Jeffrey Robbins, Section Editor</b>	
Calcium Cycling and Signaling in Cardiac Myocytes <i>Donald M. Bers</i> .....	23
Hypoxia-Induced Signaling in the Cardiovascular System <i>M. Celeste Simon, Liping Liu, Bryan C. Barnhart, and Regina M. Young</i> .....	51
<b>CELL PHYSIOLOGY, David E. Clapham, Associate and Section Editor</b>	
Bcl-2 Protein Family Members: Versatile Regulators of Calcium Signaling in Cell Survival and Apoptosis <i>Yiping Rong and Clark W. Distelhorst</i> .....	73
Mechanisms of Sperm Chemotaxis <i>U. Benjamin Kaupp, Nachiket D. Kashikar, and Ingo Weyand</i> .....	93
<b>ECOLOGICAL, EVOLUTIONARY, AND COMPARATIVE PHYSIOLOGY, Martin E. Feder, Section Editor</b>	
Advances in Biological Structure, Function, and Physiology Using Synchrotron X-Ray Imaging <i>Mark W. Westneat, John J. Socha, and Wab-Keat Lee</i> .....	119
Advances in Comparative Physiology from High-Speed Imaging of Animal and Fluid Motion <i>George V. Lauder and Peter G.A. Madden</i> .....	143

**ENDOCRINOLOGY**, *Holly A. Ingraham, Section Editor*

Estrogen Signaling through the Transmembrane G Protein–Coupled Receptor GPR30  
*Eric R. Prossnitz, Jeffrey B. Arterburn, Harriet O. Smith, Tudor I. Oprea, Larry A. Sklar, and Helen J. Hathaway* .....165

Insulin-Like Signaling, Nutrient Homeostasis, and Life Span  
*Akiko Taguchi and Morris F. White* .....191

The Role of Kisspeptins and GPR54 in the Neuroendocrine Regulation of Reproduction  
*Simina M. Popa, Donald K. Clifton, and Robert A. Steiner* .....213

**GASTROINTESTINAL PHYSIOLOGY**, *James M. Anderson, Section Editor*

Gastrointestinal Satiety Signals  
*Owais B. Chaudhri, Victoria Salem, Kevin G. Murphy, and Stephen R. Bloom* .....239

Mechanisms and Regulation of Epithelial Ca<sup>2+</sup> Absorption in Health and Disease  
*Yoshiro Suzuki, Christopher P. Landowski, and Matthias A. Hediger* .....257

Polarized Calcium Signaling in Exocrine Gland Cells  
*Ole H. Petersen and Alexei V. Tepikin* .....273

**RENAL AND ELECTROLYTE PHYSIOLOGY**, *Gerhard H. Giebisch, Section Editor*

A Current View of the Mammalian Aquaglyceroporins  
*Aleksandra Rojek, Jeppe Praetorius, Jørgen Frøkiaer, Søren Nielsen, and Robert A. Fenton* .....301

Molecular Physiology of the WNK Kinases  
*Kristopher T. Kable, Aaron M. Ring, and Richard P. Lifton* .....329

Physiological Regulation of Prostaglandins in the Kidney  
*Chuan-Ming Hao and Matthew D. Breyer* .....357

Regulation of Renal Function by the Gastrointestinal Tract: Potential Role of Gut-Derived Peptides and Hormones  
*A.R. Michell, E.S. Debnam, and R.J. Unwin* .....379

**RESPIRATORY PHYSIOLOGY**, *Richard C. Boucher, Jr., Section Editor*

Regulation of Airway Mucin Gene Expression  
*Philip Thai, Artem Loukoianov, Shinichiro Wachi, and Reen Wu* .....405

Structure and Function of the Cell Surface (Tethered) Mucins  
*Christine L. Hatrup and Sandra J. Gendler* .....431

Structure and Function of the Polymeric Mucins in Airways Mucus  
*David J. Thornton, Karine Rousseau, and Michael A. McGuckin* .....459

Regulated Airway Goblet Cell Mucin Secretion  
*C. William Davis and Burton F. Dickey* .....487

**SPECIAL TOPIC, OBESITY, Joel Elmquist and Jeffrey Flier, Special Topic Editors**

The Integrative Role of CNS Fuel-Sensing Mechanisms in Energy  
Balance and Glucose Regulation  
*Darleen Sandoval, Daniela Cota, and Randy J. Seeley* .....513

Mechanisms of Leptin Action and Leptin Resistance  
*Martin G. Myers, Michael A. Cowley, and Heike Münzberg* .....537

**Indexes**

Cumulative Index of Contributing Authors, Volumes 66–70 .....557

Cumulative Index of Chapter Titles, Volumes 66–70 .....560

**Errata**

An online log of corrections to *Annual Review of Physiology* articles may be found at  
<http://physiol.annualreviews.org/errata.shtml>

Annu. Rev. Physiol. 2008.70:119-142. Downloaded from arjournals.annualreviews.org by UNIVERSITY OF CHICAGO LIBRARIES on 02/14/08. For personal use only.